Extraordinary magnetoresistance in shunted chemical vapor deposition grown graphene devices

Adam L. Friedman,[1,2,a)] Jeremy T. Robinson,[1] F. Keith Perkins,[1] and Paul M. Campbell[1]
[1]*Code 6876, US Naval Research Laboratory, Washington, DC 20375, USA*
[2]*Code 6361, US Naval Research Laboratory, Washington, DC 20375, USA*

(Received 26 May 2011; accepted 22 June 2011; published online 14 July 2011)

We report gate tunable linear magnetoresistances (MRs) of ~600% at 12 T in metal-shunted devices fabricated on chemical vapor deposition (CVD) grown graphene. The effect occurs due to decreasing conduction through the shunt as the magnetic field increases (known as the extraordinary magnetoresistance effect) and yields an MR that is at least an order-of-magnitude higher than in un-shunted graphene devices. [doi:10.1063/1.3610565]

Known as extraordinary magnetoresistance (EMR), a large magnetoresistance (MR) enhancement is observed in metal-shunted van der Pauw (vdP) InSb and GaAs structures.[1–7] EMR is of great interest for device applications since it enables more sensitive detection at smaller scale. However, InSb and GaAs may not be suitable for scaling since their mobilities decrease substantially when device dimensions are reduced below 100 nm.[7] In contrast, graphene—a hexagonally ordered, atomically thin layer of carbon atoms that behaves as a zero-gap semiconductor—is inherently of single-atomic thickness.[8–10] Recent experiments on shunted devices of mechanically exfoliated graphene have shown a large MR, although not nearly as large as in previous studies of inhomogenous semiconductors.[11]

However, graphene exfoliation produces small, randomly shaped, and placed flakes that must be found and individually characterized for thickness, size, and position, a time-consuming process that precludes all but serial device fabrication. In contrast, it is possible to produce larger areas (in excess of sq. ft.) of greater than 95% single-layer graphene using chemical vapor deposition (CVD) on copper foils.[12] These large-area films are transferable to any arbitrary substrate and from which large numbers of nominally identical devices can be fabricated simultaneously. In this letter, we show that shunted CVD grown graphene devices exhibit linear gate-tunable EMR and that such devices are amenable to a variety of device applications.

Monolayer graphene films were grown by CVD on Cu as described in Ref. 12. The films were protected by PMMA while the Cu was removed in nitric acid. Films were transferred to a 300 nm layer of thermally grown SiO_2/Si substrate, and the PMMA was removed in acetone. Devices were fabricated with and without shunts by photolithography with Ti/Au deposited by electron-beam assisted deposition. Fig. 1(a) shows an example of shunted devices. Raman spectroscopy confirmed the presence of single-layer graphene of structural quality roughly comparable to exfoliated material (not shown). Magnetoresistance measurements were taken in a superconducting magnet system at 4.2 K using a standard low-frequency (1 Hz) lock-in technique for data acquisition. The subscript "xx" ("xy") refers to measurements with current and voltage measured with adjacent (opposite) electrodes, *i.e.*, source-drain 1-2 (1–3) and voltage probes 3-4 (2–4) in Fig. 1(a). We use the standard definition, $MR_{xx} = \Delta R_{xx}/R_{xx}(0)$, in contrast with to previous studies of shunted semiconductors.[11]

Based on the calculated components of the conductivity tensor, in zero magnetic field, current will flow through the shunt, while in a magnetic field, the current will flow around the shunt and redistribute in the graphene.[1,13] The larger the magnetic field, the more current flows through the graphene, translating to an enhancement in the MR. Fig. 1(b) displays gate voltage sweeps in different magnetic fields where this behavior is obvious. To reduce noise error caused by charging in the oxide, especially at high fields, we averaged several gate voltage sweeps. At zero field, the mobility is high, as current is flowing through the shunt, and the curve is relatively featureless with a very weak Dirac point. As the field increases, more current flows through the graphene causing a stronger Dirac point. At 10 T, the Dirac point is clearly visible and Hall minima begin to appear. As the field increases, the mobility approaches a value approximately that of the un-shunted devices tested for this study. For comparison, Fig. 1(c) displays data for an un-shunted device (Hall mobility, $\mu_H \sim 2500$ cm^2/Vs). For un-shunted devices, the curve displays a well-defined Dirac point in zero field. At high field, quantum Hall oscillations are visible and the magnitude of the signal is relatively unchanged, indicating a rather small change in mobility with increasing magnetic field.

Figure 2(a) displays the MR_{xx} for a typical shunted device for a variety of gate voltages, while Figure 2(b) displays MR_{xx} for an un-shunted device. The shunted devices show a very large, nonsaturating MR, consistently as large as ~600%, while un-shunted devices show a much smaller MR in range of ~20%, making this one of the largest MRs measured in graphene. EMR was visible in most of the devices we tested, with low 2-probe resistance (<200 Ω) being a good indicator as to whether the device would display EMR, as was also indicated in previous studies.[14] Dampened Shubnikov-de Haas oscillations (SdHOs) can be observed in the shunted devices in Fig. 2(a).

Small material inhomogeneities can amplify the MR by causing current-line distortions,[1,8,15,16] which may explain why the MR observed here is larger than that reported in

a)Author to whom correspondence should be addressed. Electronic mail: adam.friedman@nrl.navy.mil.

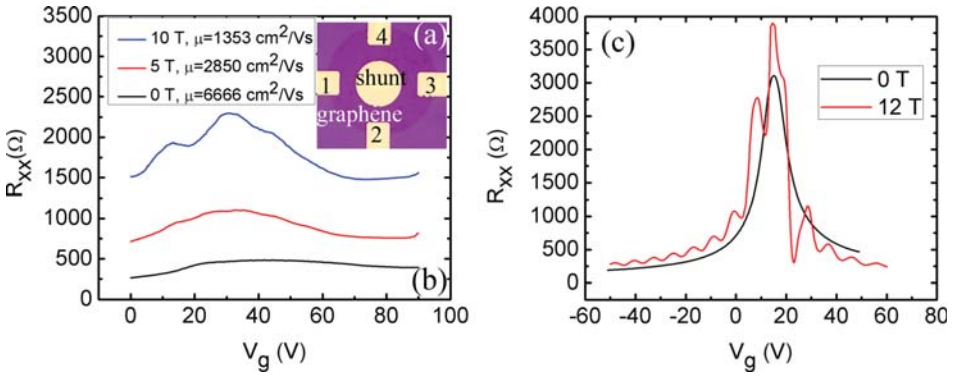

FIG. 1. (Color online) (a) Optical image of a shunted graphene device. (b) R_{xx} vs. V_g for a shunted device at different fields. The mobility decreases for higher fields, while the Dirac point gets sharper and quantum Hall oscillations become visible indicating shunting behavior. (c) R_{xx} vs. V_g for an un-shunted device at different fields. There is a little change in mobility at the Dirac point as the field increases and Hall oscillations are very clear. Applied current in all cases was 10 μA.

Ref. 11, which used single-crystal exfoliated flakes of graphene with presumably few inhomogeneities. CVD graphene is known to have defects such as domain boundaries,[17] which may be advantageous to enhancing MR. This suggests CVD graphene offers an advantage over exfoliated graphene because growth parameters, such as temperature or pressure, can be used to tune these types of defects.[18] In addition, in Fig. 2(a), we see that the MR response is strongly linear and nonsaturating. This behavior is explained by models that predict linear, nonsaturating MR in a material composed of conducting and semiconducting regions.[8,13,15] The inset of Fig. 2(a) displays the slope of the MR line, which is the sensitivity of the device, as a function of gate voltage. Similar to past studies,[11] the sensitivity is gate tunable and the maximum in sensitivity corresponds to the Dirac point of the graphene.

Shunted graphene devices may also have potential applications as Hall sensors. Fig. 3 shows the R_{xy} vs. field for a variety of gate voltages and Fig. 3(b) shows a close-up of the locations in magnetic field where the minimum values of resistance occurred. Because the lock-in measures the magnitude of the signal, this minimum is actually the x-axis intercept of the R_{xy} line. The position of the minimum is also gate tunable. We attribute this minimum in R_{xy} at nonzero field to a breaking in symmetry caused by extrinsic factors, such as surface contaminants remaining from the device fabrication process. For shunted devices, resist residue trapped beneath the shunt cannot be removed by any post-process cleaning. It is likely that with purposeful chemical doping of the graphene surface, we may be able to control the location of the R_{xy} minimum.

Room temperature measurements (Fig. 3(c)) were made with two fixed-field permanent magnets ($\pm$0.37 T and $\pm$0.55 T). There is virtually no difference in the resistance between 4.2 K and room temperature. This is not unexpected, as the mobility of graphene, upon which the resistance depends, is nearly constant over this temperature range.[9,13,19] This suggests that MR and Hall devices made from CVD graphene would operate as well at room temperature as at 4.2 K.

It is possible to imagine numerous device applications that utilize the linear EMR and tunable minimum in the Hall resistance. This would enable small, highly sensitive, easily calibrated magnetic sensors, which are of great interest in nanomagnetism where it is necessary to measure small signals.[20,21] The Johnson noise, which is the dominant noise source in these devices,[11] limited power signal is given by $SNR_{power} = 10log_{10}\{[I_{in}(dR/dH)_{Bias}\Delta H]^2/4k_BT[R_{out}(H)]_{HBias}\Delta f\}$. Here, I_{in} is the applied current, $(dR/dH)_{Bias}$ is the sensitivity at H_{bias}, which is the field at which the signal is measured, T is the temperature in Kelvin, $[R_{out}(H)]_{HBias}$ is the resistance at H_{bias}, k_B is Boltzmann's constant, and Δf is the detection bandwidth. For a typical device in our study at 50 mT and 1 GHz, SNR_{Power} ~27 dB, which is comparable to other devices previously reported.[11]

In conclusion, we have shown that shunted CVD grown graphene devices display EMR. The sensitivity of such devices is tunable by varying V_g. There are numerous applications for such devices, including magnetic field sensors and memory read-heads. However, it is not yet clear how the apparent need for slight inhomogeneities in the graphene will reconcile with the need for higher mobility, as mobility coupled the cleanliness and defectiveness of the graphene. Nonetheless, such devices have the important advantage of exploiting graphene's innate properties without requiring any modification to the material, *e.g.,* induced bandgap. Devices fabricated from CVD graphene could be manufactured on a vastly larger scale than from exfoliated graphene and in any geometry desired.

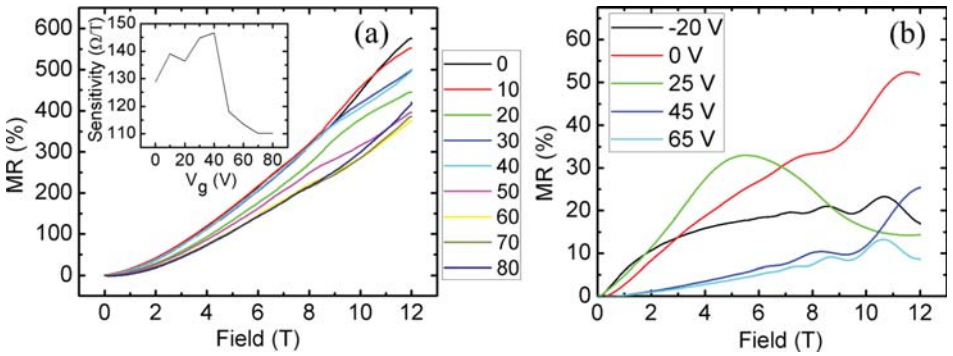

FIG. 2. (Color online) (a) MR for a typical shunted device showing a ~600% change. The inset shows the sensitivity of the device. The slight oscillations are attributed to SdHO. (b) MR for a typical un-shunted device showing a much smaller change. The SdHO are much more pronounced.

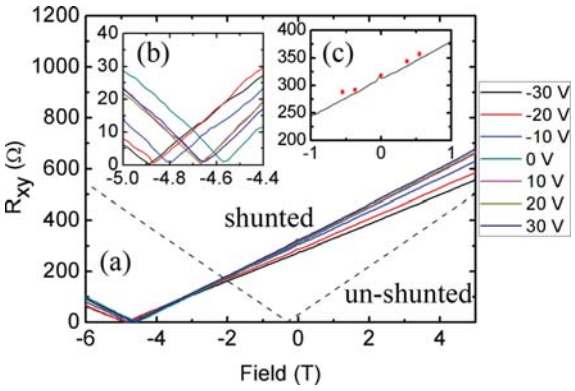

FIG. 3. (Color online) (a) R_{xy} vs. Field for various gate voltages for an externally shunted device. The black dashed line shows an un-shunted device. The minimum (intercept) moves further to the left for more chemically doped devices. (b) A close-up of the minimum. (c) A comparison of low temperature (4.2 K = black line) to room temperature (293 K = red points) data for resistance vs. field. There is a little resistance change.

Note added in proof: While in proof, a manuscript with results similar to our own (Lu, *et al*. Nano Lett. (2011) doi: 10.1021/nl201538m) was published with a received date of May 9, 2011. We note that a draft of our manuscript was first submitted for review on August 12, 2010.

The authors thank K. Bussman of NRL for helpful discussions.

[1]S. A. Solin, T. Thio, D. R. Hines, and J. J. Heremans, Science **289**, 1530 (2000).
[2]S. A. Solin, D. R. Hines, A. C. H. Rowe, J. S. Tsai, Y. A. Pashkin, S. J. Chung, N. Goel, and M. B. Santos, Appl. Phys. Lett. **80**, 4012 (2002).
[3]C. H. Moller, O. Kronenewerth, D. Grundler, W. Hansen, Ch. Hyen, and D. Heitmann, Appl. Phys. Lett. **80**, 3988 (2002).
[4]M. Hoener, O. Kronenwerth, C. Heyn, D. Grundler, and M. Holz, J. Appl. Phys. **99**, 036102 (2006).
[5]C.-B. Rong, H.-W. Zhang, J.-R. Sun, and B.-G. Shen, Appl. Phys. Lett. **89**, 052503 (2006).
[6]A. S. Troup, D. G. Hasko, J. Wunderlich, and D. A. Williams, Appl. Phys. Lett. **89**, 022116 (2006).
[7]S. A. Solin, D. R. Hines, J. S. Tsai, Y. A. Pashkin, S. J. Chung, N. Goel, and M. B. Santos, IEEE Trans. Magn. **38**, 89 (2002).
[8]A. L. Friedman, J. L. Tedesco, P. M. Campbell, J. C. Culbertson, E. Aifer, F. K. Perkins, R. L. Myers-Ward, J. K. Hite, C. R. Eddy, G. G. Jernigan, and D. K. Gaskill, Nano Lett. **10**, 3962 (2010).
[9]Z. Jiang, Y. Zhang, Y.-W. Tan, H. L. Stormer, and P. Kim, Solid State Commun. **143** 14 (2007).
[10]A. K. Geim and K. S. Novoselov, Nature Materials. **6**, 183 (2007).
[11]S. Pisana, P. M. Braganca, E. E. Marinero, and B. A. Gurney, Nano Lett. **10**, 341 (2010).
[12]X. Li, W. Cai, J. An, S. Kim, J. Nah, D. Yang, R. Piner, A. Velamakanni, I. Jung, E. Tutuc, S. K. Banerjee, L. Colombo, and R. S. Ruoff, Science **324**, 1312 (2009).
[13]T. H. Hewett and F. V. Kusmartsev, ArXiv:1007.5452v1 [cond-mat.mtrl-sci] (2010).
[14]S. A. Solin, Proc. SPIE **7679**, 76790B (2010).
[15]J. Hu and T. F. Rosenbaum, Nature Mater. **7**, 697 (2008).
[16]C. Herring, J. Appl. Phys. **31** 1939 (1960).
[17]X. Li, Y. Zhu, W. Cai, M. Borysiak, B. Han, D. Chen, R. D. Piner, L. Colombo, and R. S. Ruoff, Nano Lett. **12**, 4359 (2009).
[18]X. Li, C. W. Magnuson, A. Venugopal, J. An, J. W. Suk, B. Han, M. Borysiak, W. Cai, A. Velamakanni, Y. Zhu, L. Fu, E. M. Vogel, E. Voelk, L. Colombo, and R. S. Ruoff, Nano Lett. **10**, 4328 (2010).
[19]K. S. Novoselov, Z. Jiang, Y. Zhang, S. V. Morozov, H. L. Stormer, U. Zeitler, J. C. Maan, G. S. Boebinger, P. Kim, and A. K. Geim, Science **9**, 1379 (2007).
[20]F. Meier, L. Zhou, J. Wiebe, and R. Wiesendagner, Science **320**, 82 (2008).
[21]A. L. Friedman, H. Chun, Y. J. Jung, D. Heiman, E. R. Glaser, and L. Menon, Phys. Rev. B **81**, 115461 (2010).